Hindawi
Mathematical Problems in Engineering
Volume 2021, Article ID 3716033, 9 pages
https://doi.org/10.1155/2021/3716033

Research Article

Compound Fault Diagnosis of Gearbox Based on RLMD and SSA-PNN

Shitong Liang and Jie Ma

School of Mechatronics Engineering, Beijing Information Science and Technology University, Beijing, China

Correspondence should be addressed to Jie Ma; mjbeijing@163.com

Received 6 July 2021; Accepted 18 September 2021; Published 29 September 2021

Academic Editor: Yong Chen

In order to solve the difficulty in the classification of gearbox compound faults, a gearbox fault diagnosis method based on the sparrow search algorithm (SSA) improved probabilistic neural network (PNN) is proposed. Firstly, the gearbox fault signal is decomposed into a series of product functions (PFs) by robust local mean decomposition (RLMD). Then, the permutation entropy of PFs, which contains much fault information, is calculated to construct the feature vector and input it into the SSA-PNN model. The experimental results show that compared with the traditional fault diagnosis methods based on EMD-BP and EEMD-PNN, the gearbox fault diagnosis method based on RLMD and SSA-PNN has higher diagnosis accuracy.

1. Introduction

The gearbox is the core component of mechanical equipment, and its running state is closely related to the safe operation of the equipment. Gearbox faults often occur as multiple faults in practical engineering applications and may cause abnormal operation of the equipment system and even lead to significantly reduced service life and degraded property. Therefore, compound fault diagnosis of the gearbox plays an important role in the safety maintenance of the mechanical system. Vibration signal analysis is one of the common analysis methods of gearbox fault diagnosis [1]. Vibration signals can be obtained through the contact sensor installed on the machine shell or base or through the airborne acoustic array sensor. However, in actual working conditions, the environmental background noise is large, and the fault impact characteristics of vibration signals are submerged in the cluttered noise, making it difficult to obtain fault information from original signals with the naked eye. Signal decomposition is one of the effective methods to deal with vibration signals. The ensemble empirical mode decomposition (EEMD) method [2] is widely used for feature extraction of fault signals. By adding Gaussian white noise when dealing with decomposed signal EMD, EEMD uses the binary filter bank characteristics of the EMD filter to fill the whole time-frequency space to reduce mode mixing. However, the added noise may not be completely eliminated and will cause signal reconstruction error [3]. To solve modal aliasing and end effect, Liu proposed a robust local mean decomposition (RLMD) method [4]. Yan [5] reconstructed the PFs obtained from RLMD of the signal and used the *K*-means++ clustering method to cluster the fault features. The effectiveness of this method was verified by simulation and experiments.

In the current fault diagnosis methods [6], the BP neural network is the most widely used, but it also has many shortcomings, such as the tendency to fall into the local extremum because of the dependence on the initial network weight, slow convergence, and so on. Compared with the BP neural network, the probabilistic neural network [7] converges faster and has higher diagnosis accuracy. Wang [8] used multiscale entropy (MSE) to extract fault features from signals and then input them into PNN. The results showed good fault diagnosis ability of the MSE-PNN model. Di [9] used EEMD to decompose signals into multiple IMFs, then took the energy as the feature vector, and inputted it into PNN. It was proved that this method has high recognition accuracy. However, the smoothing factor in PNN can only

be selected by artificial experience without a fixed method. Among swarm intelligence optimization algorithms [10–12], the sparrow search algorithm (SSA) [13] with strong search ability and fast convergence speed [14] is the best, and therefore, it can be used in the adaptive selection of smoothing factors to make them reflect the characteristics of the sample to the maximum extent. Accordingly, a gearbox fault diagnosis method based on RLMD and PNN optimized by SSA is proposed in this paper.

2. Robust Local Mean Decomposition

2.1. Local Mean Decomposition. The local mean decomposition (LMD) method [15] is an adaptive time-frequency representation method through iterative operation and can decompose a signal into a series of product functions (PFs), each of which is the product of the FM signal and the envelope signal. If the given original signal is $x(t)$, the LMD algorithm steps are as follows.

Step 1. All local maxima and minimums of the signal $x(t)$ are obtained. The extreme points are represented by e_w, and the corresponding extremes are marked as $x(e_w)$ with $w = 1, 2, 3, \ldots$

Step 2. The local mean $m^0(t)$ and local amplitude $a^0(t)$ are preprocessed according to formulas (1) and (2), and then, the smoothing algorithm is used to postprocess $m^0(t)$ and $a^0(t)$ for the smoothed local mean $m(t)$ and local amplitude $a(n)$:

$$m^0(t) = \frac{x(e_w) + x(e_{w+1})}{2}, \tag{1}$$

$$a^0(t) = \frac{|x(e_w) - x(e_{w+1})|}{2}. \tag{2}$$

Step 3. The initial local average $x(t)$ is removed from the original signal $m_{11}(t)$, and the estimated zero-mean signal $h_{11}(t)$ is obtained as

$$x(t) - m_{11}(t) = h_{11}(t). \tag{3}$$

Step 4. The estimated FM signal $s_{11}(t)$ is obtained by dividing $h_{11}(t)$ by $a_{11}(t)$, that is,

$$s_{11}(t) = \frac{h_{11}(t)}{a_{11}(t)}. \tag{4}$$

After the LMD, if the signal $s_{11}(t)$ does not meet the requirements, that is, it is not a pure FM signal, and $s_{11}(t)$ will be regarded as a new signal to repeat Steps (1) to (4) P times until the conditions in formula (5) are satisfied:

$$\lim_{P \longrightarrow \infty} a_{1p}(t) = 1. \tag{5}$$

Step 5. When formula (5) is established, the FM signal $s_1(t)$ which meets the requirements can be calculated by formula (6), and the envelope signal $a_1(t)$ can be calculated by formula (7). The first product function $PF_1(t)$ can be obtained by multiplying $s_1(t)$ with $a_1(t)$:

$$s_1(t) = s_{1P}(t), \tag{6}$$

$$a_1(t) = \prod_{j=1}^{P} a_{1j}(t). \tag{7}$$

Step 6. The residual signal $u_1(t)$ is obtained by subtracting $PF_1(t)$ from the original signal. Steps (1) to (5) are repeated Q times until $u_1(t)$ is a constant or nonoscillatory function, and then, the original signal can be represented by the sum of multiple product functions and residual components:

$$x(t) = \sum_{i=1}^{Q} PF_i(t) + u_Q(t). \tag{8}$$

2.2. Robust Local Mean Decomposition. Because of mode aliasing and end effect of LMD, Liu proposed RLMD. The improvements are as follows.

Step 1. Boundary condition optimization: the mirror expansion algorithm [16] is used to find the symmetrical points of the signal with respect to the endpoints at both ends.

Step 2. Envelope estimation: for the value λ^* that needs to be selected by artificial experience, Liu creatively uses a method based on statistical theory:

$$\lambda^* = \mathrm{odd}(\mu_s + 3 \times \delta_s). \tag{9}$$

In the formula, $\mathrm{odd}(\cdot)$ is the nearest odd number of the input, μ_s is the center of the step, and δ_s is the standard deviation of the step.

Step 3. Stop criteria filter: the objective function $f(x)$ is minimized:

$$f(x) = \mathrm{RMS}(z(t) + \mathrm{EK}z(t)), \tag{10}$$

where the zero-baseline envelope signal $z(t) = a(t) - 1$ and $\mathrm{RMS}(\cdot)$ and $\mathrm{EK}(\cdot)$ are given by formulas (11) and (12) as follows:

$$\mathrm{RMS} = \sqrt{\frac{1}{N}\sum_{t=1}^{N}(z(t))^2}, \tag{11}$$

$$\mathrm{EK} = \frac{(1/N)\sum_{t=1}^{N}(z(t) - \overline{z})^4}{\left((1/N)\sum_{t=1}^{N}(z(t) - \overline{z})^2\right)^2} - 3, \tag{12}$$

where $\overline{z}$ is the average of $z(n)$.

2.3. Simulation Experiment and Analysis. In order to verify the superiority of RLMD, a composite signal is simulated:

$$\begin{cases} x_1(t) = \cos(300\pi t), \\ x_2(t) = \sin(1600\pi t), \\ x_3(t) = 0.5randn(1,n), n = \text{length}(t), \\ x(t) = x_1(t) + x_2(t) + x_3(t). \end{cases} \tag{13}$$

The sampling frequency is 20480 Hz, the number of sampling points is 4096, and the time domain waveforms of each component and composite signal are shown in Figure 1.

The first four PFs and IMFs obtained by simultaneous RLMD and EMD of the signal are shown in Figures 2 and 3.

Figure 2 shows that the PF1 component mainly corresponds to function $x_2(t)$, and the PF2 component mainly corresponds to function $x_1(t)$, while in Figure 3, all components are affected by modal aliasing, resulting in that their significance is not obvious. Therefore, the superiority of the RLMD method is shown.

3. PNN Model Optimized by SSA

3.1. Sparrow Search Algorithm. Sparrow search algorithm is a new swarm intelligence optimization algorithm, which simulates the foraging behavior of the sparrow population, and in this algorithm, the sparrow population is divided into discoverers and participators. The population X with the number of sparrows n is expressed by formula (13):

$$X = \begin{bmatrix} x_{1,1} & x_{1,2} & \cdots & x_{1,d} \\ x_{2,1} & x_{2,2} & \cdots & x_{2,d} \\ \vdots & \vdots & \vdots & \vdots \\ x_{n,1} & x_{n,2} & \cdots & x_{n,d} \end{bmatrix}. \tag{14}$$

In the formula, d is the dimension of the parameter to be optimized and n is the number of populations. Then, the fitness values of all sparrows can be expressed as formula (14):

$$F_X = \begin{bmatrix} f([\, x_{1,1} \;\; x_{1,2} \;\; \cdots \;\; x_{1,d} \,]) \\ f([\, x_{2,1} \;\; x_{2,2} \;\; \cdots \;\; x_{2,d} \,]) \\ \vdots \\ f([\, x_{n,1} \;\; x_{n,2} \;\; \cdots \;\; x_{n,d} \,]) \end{bmatrix}. \tag{15}$$

The iterative formula of the discoverer's position is expressed as formula (15):

$$X_{i,j}^{t+1} = \begin{cases} X_{i,j}^{t} \cdot \exp\left(-\dfrac{i}{\alpha \cdot \text{iter}_{\max}}\right), & \text{if } R_2 < ST, \\ X_{i,j}^{t} + Q \cdot L, & \text{if } R_2 \geq ST, \end{cases} \tag{16}$$

where t is the number of iterations, $\text{iter}_{\max}$ is the maximum number of iterations, and Q is a random number, which obeys normal distribution. The maximum value of j is the dimension d of the parameter to be optimized; L is a row matrix with the length d, and the element is 1; R_2 and ST represent early warning value and safety value, respectively.

The iterative formula of the participant's position is expressed as formula (16):

$$X_{i,j}^{t+1} = \begin{cases} Q \cdot \exp\left(\dfrac{X_{\text{worst}} - X_{i,j}^{t}}{i^2}\right), & \text{if } i > \dfrac{n}{2}, \\ X_{p}^{t+1} + \left|X_{i,j}^{t} - X_{P}^{t+1}\right| \cdot A^{+} \cdot L, & \text{otherwise}, \end{cases} \tag{17}$$

where X_p and X_{worst} represent the global best location and global worst location found by the discoverer so far, respectively. A is a row matrix with the length d, the element is set as 1 or -1 randomly, and $A^{+} = A^{T}(AA^{T})^{-1}$.

In this paper, the sum of the classification error rate of the training set and the classification error rate of the test set is used as the fitness value.

3.2. Probabilistic Neural Network. A probabilistic neural network [17] is a kind of neural network that can be used for pattern classification, and its essence is a parallel algorithm based on the Bayesian minimum risk criterion. It has the characteristics of a simple learning process, fast training speed, more accurate classification, good fault tolerance, and so on.

Probabilistic neural networks are generally divided into four layers, namely, input layer, pattern layer, summation layer and output layer.

The input layer is used to input the high-dimensional fault feature matrix for analysis. The number of input layers is affected by the dimension of the fault feature matrix.

The pattern layer connects with the input layer through the connection weight. It calculates the matching degree, that is, the similarity between the input feature vector and each pattern in the training set, and then inputs it into the activation function. The result is the output of the pattern layer.

The summation layer is responsible for connecting the pattern layer units of each class. The number of neurons in this layer is consistent with the number of fault types.

The output layer classifies the fault type by outputting the maximum value in the summation layer.

The basic model of PNN is shown in Figure 4.

4. Compound Fault Diagnosis of the Gearbox by RLMD-SSA-PNN

In order to solve the problems of compound fault diagnosis of the gearbox, an improved PNN algorithm based on RLMD and SSA is proposed in this paper, and the specific steps are as follows.

Step 1. The signal is decomposed by RLMD, and a series of PFs are obtained. The number of PFs containing much fault information is judged by the correlation coefficient, and the permutation entropy of each effective PF is calculated. After that, the high-dimensional fault characteristic matrix is constructed.

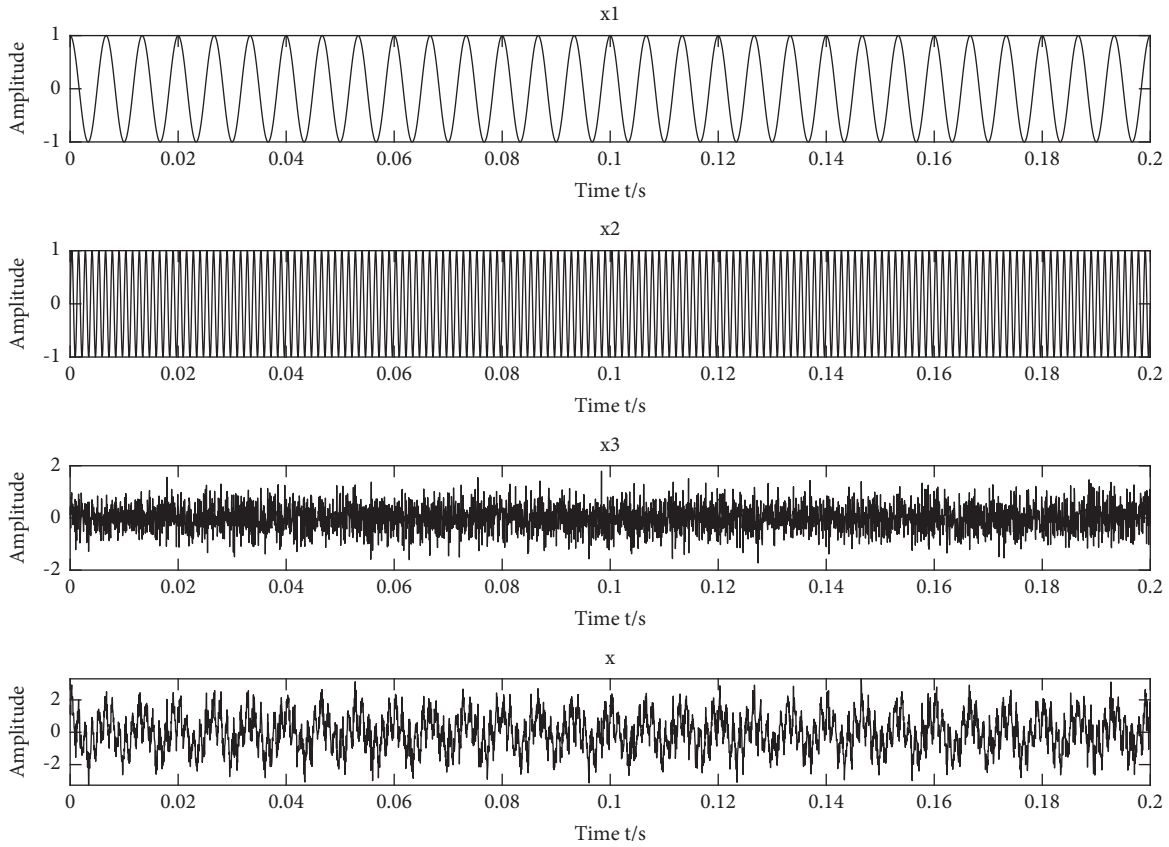

Figure 1: Each component and coincidence signal waveform.

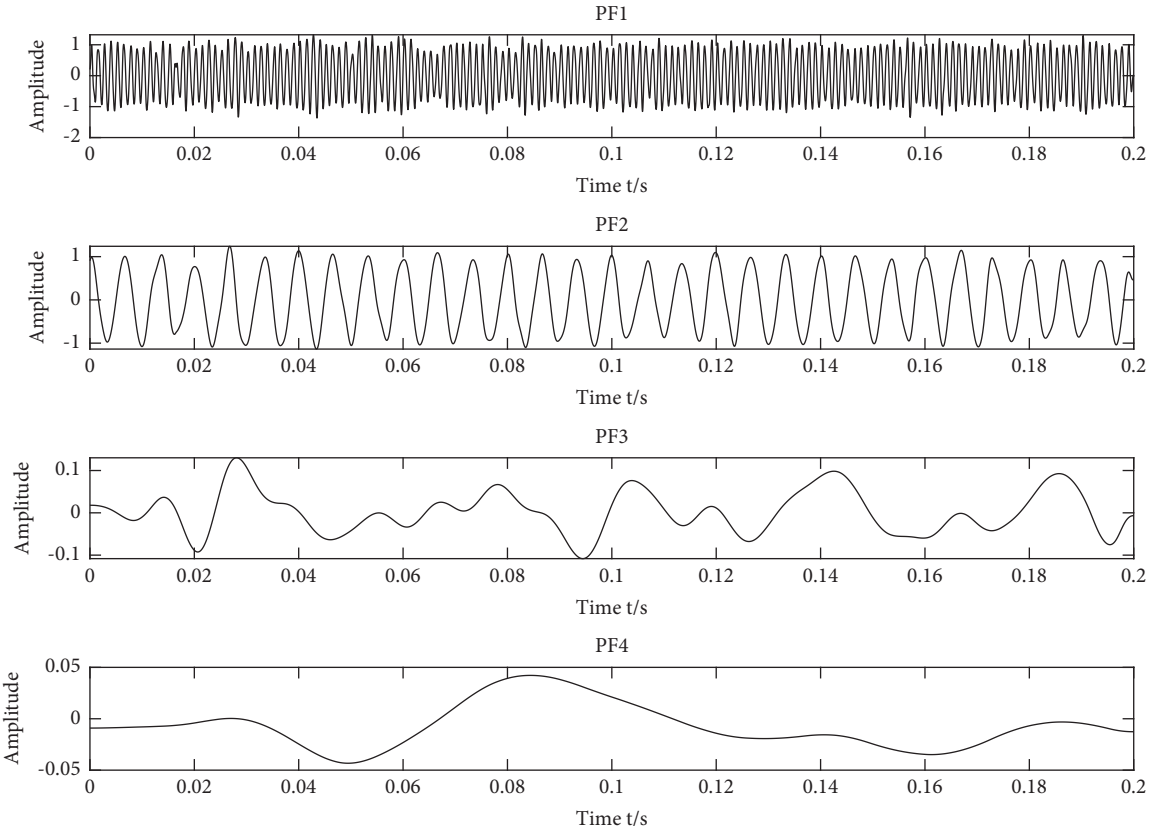

Figure 2: PFs waveform.

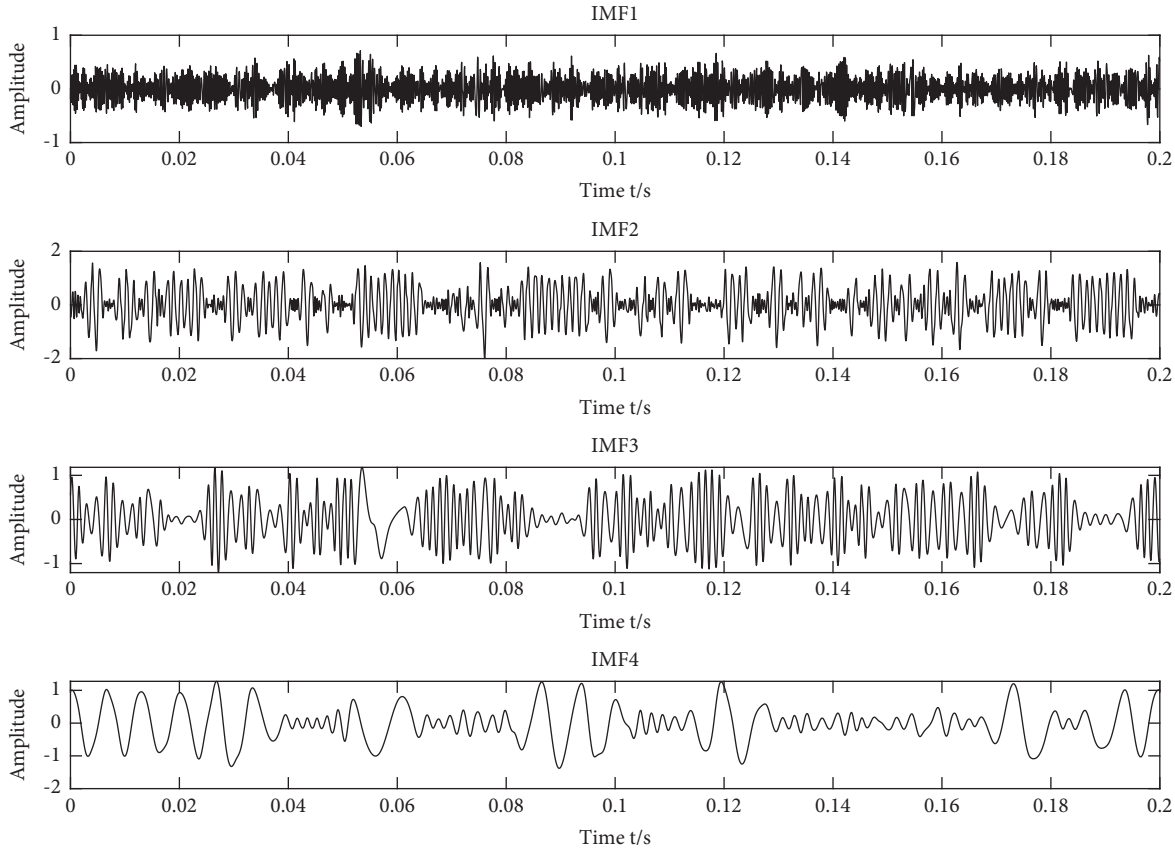

Figure 3: IMFs waveform.

Step 2. The fault characteristic matrix is divided into the training set and test set, which are then labeled.

Step 3. Parameters in the sparrow search algorithm are set, such as the number of populations, maximum number of iterations, and upper and lower boundaries of the search (the range of smoothing factors).

Step 4. The training set and its label are input into the SSA-PNN model for training, making the model find the optimal value of the smoothing factor, and then, the test set and its label are input for the test.

5. Experiment and Analysis

5.1. Data Acquisition. This paper used the gearbox test platform of the Ministry of Education Key Laboratory in Beijing Information Science and Technology University to collect data. The test bench includes an acceleration sensor, conditioning circuit, acquisition instrument, planetary gearbox test platform, and computer.

The range of speed adjustment is 1140–2220 rpm, and the step size is 120 rpm. Five types of data are included, namely, the normal planetary gear, planetary gear tooth fracture, planetary gear tooth surface wear, planetary gear tooth fracture plus tooth surface wear, and planetary gear tooth fracture plus rolling body missing. Each type of data is collected three times, with the sampling frequency of 20480 Hz and the sampling time of each collection being 3s. The length of each collected signal is 61440. The data used in this paper are the fault data under the speed of 1500 r/min, and the time domain diagram of each type is shown in Figure 5.

5.2. Construction of High-Dimensional Fault Characteristic Matrix. Considering the computational cost and efficiency, each collected signal is divided into 30 short samples, with the length of each sample being 2048, and there are a total of 90 short samples for each type of data. Sixty of them are randomly selected as the training set, and the remaining 30 are chosen as the test set. Since there are 5 data types in the experiment, a total of 300 short samples are used as the training set, and 150 samples are selected as the test set. The labels of the normal type, broken tooth type, wear type, wear and broken tooth type, broken tooth type, and rolling body missing type are 1, 2, 3, 4, and 5, respectively.

Taking the fault signal of tooth breaking of the planetary gear as an example, this paper shows the decomposition of a short sample with a length of 2048 by RLMD to get multiple PFs, as shown in Figure 6.

The above six PFs' components are obtained after the fault signal of planetary gear tooth breaking is decomposed by RLMD. In fact, there are still meaningless components in the PFs' components of the signal after RLMD. Taking these components as feature elements will cause interference and reduce the recognition accuracy of the recognition

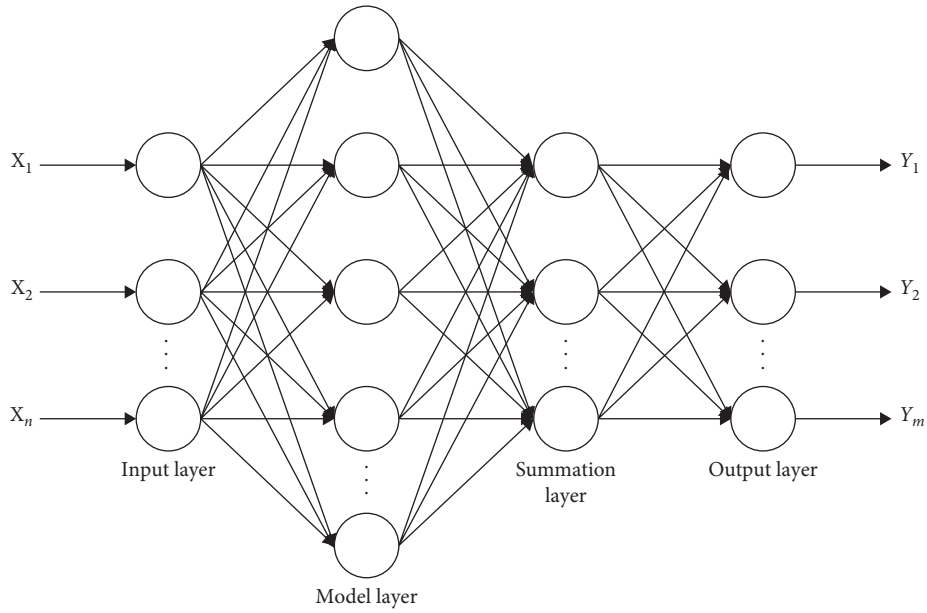

Figure 4: Schematic diagram of the PNN structure.

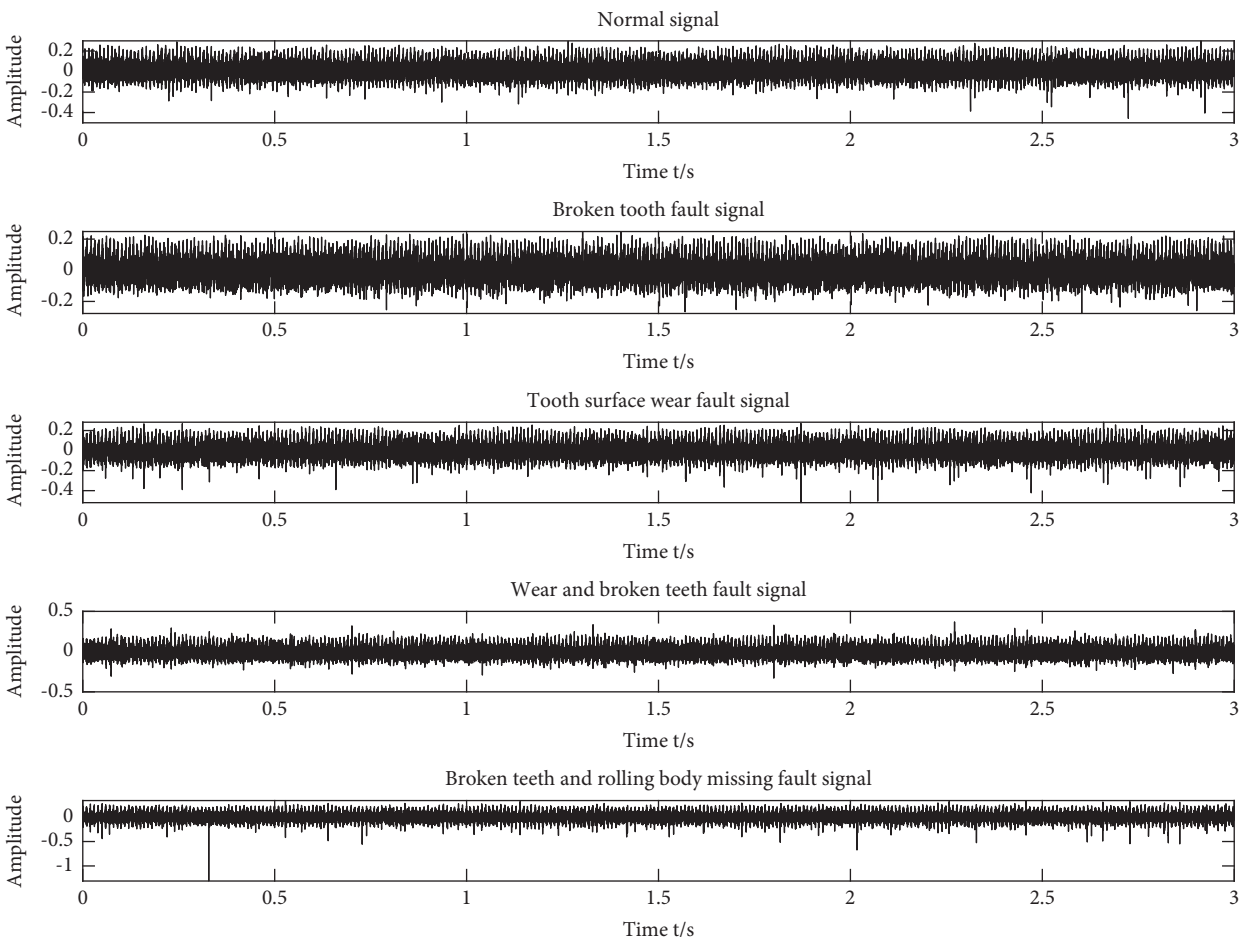

Figure 5: Five types of data waveform.

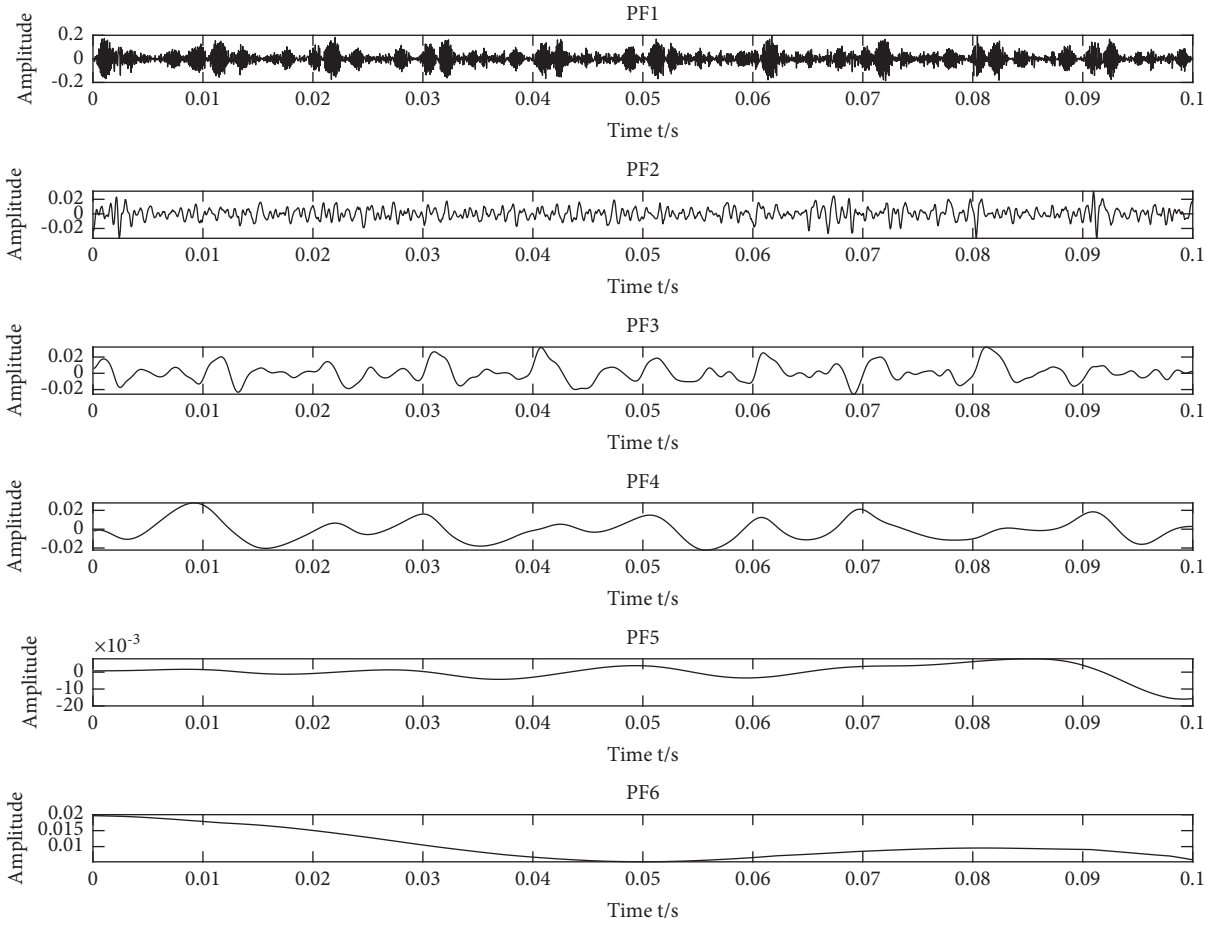

Figure 6: Each PF waveform.

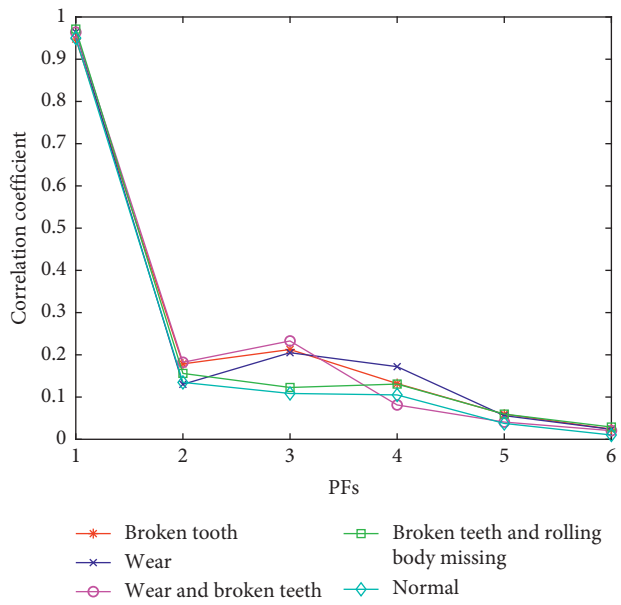

Figure 7: Correlation coefficient between each PF and the original signal.

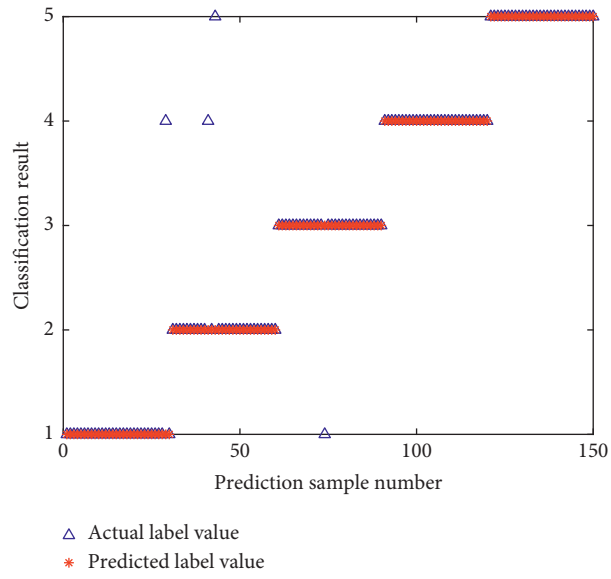

Figure 8: Classification result of the SSA-PNN model.

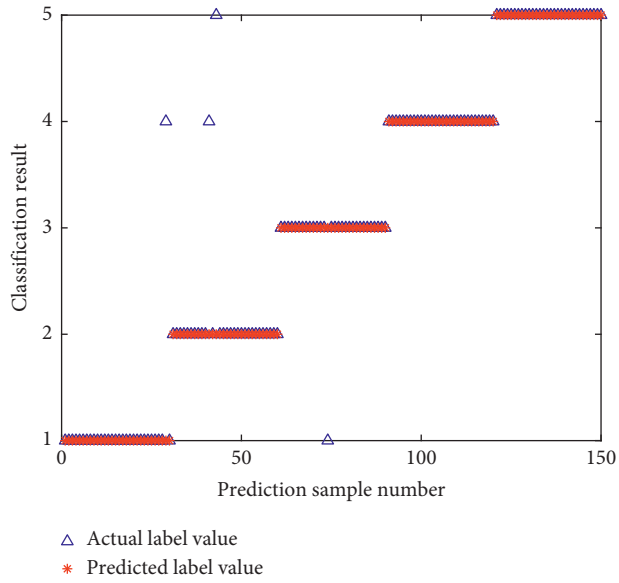

Figure 9: Classification result of the EMD-BP model.

algorithm. Therefore, it is necessary to use the correlation coefficient method to filter out the unimportant PFs components.

The correlation coefficients of PFs' components of five types of data decomposed by RLMD are calculated, as shown in Figure 7. It can be seen that the correlation coefficients of the PFs after PF4 are all lower than 0.1, which indicates that the latter PFs can hardly reflect the fault characteristics of the original signal, and therefore, the first four PFs are retained as effective components. Then, the permutation entropy of these four PFs is calculated, and the fault characteristic matrix of 450×4 is obtained.

5.3. Experimental Results and Analysis. The fault characteristic matrix is inputted into the SSA-PNN model, and the result is shown in Figure 8. It is shown that, in the 150 short samples of the test set, only 4 short samples have classification errors, including the diagnosis of the normal type as wear plus broken teeth, the diagnosis of the broken teeth as wear plus broken teeth, the diagnosis of the broken teeth as rolling body missing plus broken teeth, and the diagnosis of the wear as the normal type, and the overall classification accuracy reaches 97.33%.

In order to verify the superiority of the proposed method, it is compared with other methods. This paper uses

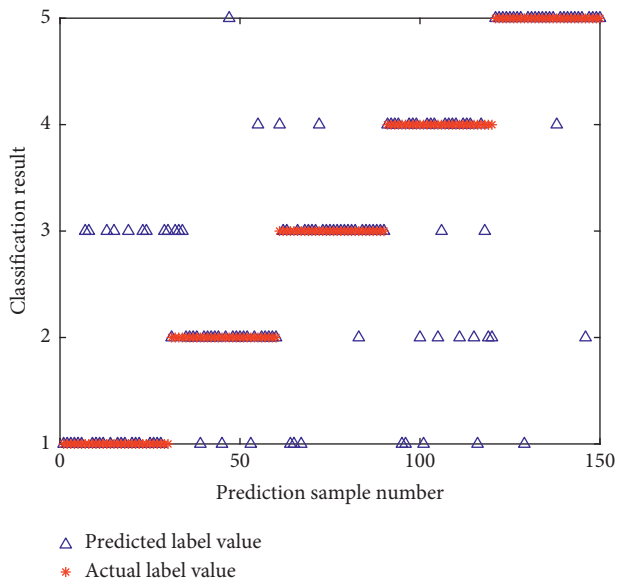

Figure 10: Classification result of the EEMD-PNN model.

EMD to decompose the signal, then takes the first four IMFs as sensitive components, and also uses permutation entropy as the index to construct the feature matrix, which is input into the BP model. The classification results of the EM-BP model are shown in Figure 9. It is shown that there are 38 classification errors in the short samples of the test set, and the classification accuracy is only 74.67%. Similarly, the EEMD-PNN model is used, and its fault classification results are shown in Figure 10. It can be seen that there are 13 classification errors in the short samples of the test set, and the classification accuracy is 91.33%.

6. Conclusions

In this paper, a gearbox fault diagnosis method based on robust mean decomposition and SSA improved PNN model is proposed. This method can effectively adaptively select the smoothing factors in the PNN model so as to achieve a good classification effect. Besides, it has higher diagnosis accuracy than EMD-BP, EEMD-PNN, and other classification methods and is suitable for fault diagnosis of the gearbox.

Data Availability

The data used to support the findings of this study are available from the corresponding author upon request.

Conflicts of Interest

The authors declare that there are no conflicts of interest regarding the publication of this paper.

Acknowledgments

This work was supported by the National Natural Science Foundation of China (Grant no. 61973041) and National Key Research and Development Program of China (Grant no. 2019YFB1705403).

References

[1] G. Yu, T. Lin, Z. Wang, and Y. Li, "Time-reassigned multisynchrosqueezing transform for bearing fault diagnosis of rotating machinery," *IEEE Transactions on Industrial Electronics*, vol. 68, no. 2, pp. 1486–1496, 2021.

[2] H. H. Wu, E. Norden, and Huang, "Ensemble empirical mode decomposition: a noise-assisted data analysis method," *Advances in Adaptive Data Analysis*, vol. 1, no. 1, pp. 1–41, 2009.

[3] C. Ma, S. H. Wang, and X. L. Xu, "Fault diagnosis for rolling bearing by using acoustic array based on EEMD," *Journal of Electronic Measurement and Instrument*, vol. 31, no. 9, pp. 1379–1384, 2017.

[4] Z. Liu, Y. Jin, M. J. Zuo, and Z. Feng, "Time-frequency representation based on robust local mean decomposition for multicomponent AM-FM signal analysis," *Mechanical Systems and Signal Processing*, vol. 95, pp. 468–487, 2017.

[5] S. T. Yan, Y. G. Zhou, and Y. B. Rrn, "Bearing fault diagnosis method based on RLMD and Kmeans++," *Journal of Mechanical Transmission*, vol. 45, no. 2, pp. 163–170, 2021.

[6] J. Ma and J. A. Xu, "Fault prediction algorithm for multiple mode process based on reconstruction technique," *Mathematical Problems in Engineering*, vol. 2015, Article ID 348729, 8 pages, 2015.

[7] L. X. Yang and Y. L. Zhu, "High voltage circuit breaker fault diagnosis of probabilistic neural network," *Power System Protection and Control*, vol. 43, no. 10, pp. 62–67, 2015.

[8] W. Wang, B. Zhou, and R. M. Zhang, "Fault diagnosis of rolling bearing in mechanical equipment based on MSE and PNN," *China Plant Engineering*, vol. 15, pp. 145–147, 2020.

[9] H. Di, W. L. Sun, and Y. Z. Wu, "Research on fault diagnosis for wind turbine based on EEMD and PNN," *Machinery design and manufacture*, vol. 6, pp. 105–108, 2020.

[10] S. Mirjalili, S. M. Mirjalili, and A. Lewis, "Grey wolf optimizer," *Advances in Engineering Software*, vol. 69, no. 3, pp. 46–61, 2014.

[11] S. Seyedali, "Dragonfly algorithm: a new meta-heuristic optimization technique for solving single-objective, discrete, and multiobjective problems," *Neural Computing and Applications*, vol. 27, no. 4, pp. 1053–1073, 2016.

[12] S. Saremi, S. Mirjalili, and A. Lewis, "Grasshopper optimisation algorithm: theory and application," *Advances in Engineering Software*, vol. 105, pp. 30–47, 2017.

[13] J. K. Xue, *Research and Application of A Novel Swarm Intelligence Optimization Technique: Sparrow Search Algorithm*, Donghua University, Shanghai, China, 2020.

[14] Y. L. Li, S. Q. Wang, and Q. R. Chen, "A comparative study of several new swarm intelligence optimization algorithms," *Computer Engineering and Applications*, vol. 56, no. 22, pp. 1–12, 2020.

[15] S. Q. Chen, Z. K. Peng, and P. Zhuo, "Review of signal decomposition theory and its applications in machine fault diagnosis," *Journal of Mechanical Engineering*, vol. 56, no. 17, pp. 91–107, 2020.

[16] G. Rilling, P. Flandrin, and P. Goncalves, "On empirical mode decomposition and its algorithms," in *Proceedings of the 6th IEEE/EURASIP Workshop on Nonlinear Signal and Image Processing*, Grado, Italy, 2003.

[17] F. Specht Donald, "Probabilistic neural networks," *Pergamon*, vol. 3, no. 1, 1990.